# NEW DEVELOPMENTS IN VHF/UHF ANTENNAS

F.M. Landstorfer

Technical University of Munich, Germany

## INTRODUCTION

The VHF/UHF-range as defined in this paper covers the frequency band of approximately 30 MHz to 1 GHz. Whereas to some extent arbitrary, the band limits do have some physical meaning.

At frequencies lower than 30 MHz antenna dimensions generally are much smaller than a wavelength; as a consequence only simple forms of antennas are used and their directivity is limited to that of a dipole or a loop.

At frequencies above 1 GHz with antenna dimensions of many wavelengths, antennas are designed on the basis of optical models and high values of directivity and gain are feasible.

The VHF/UHF-range is characterised by the fact that the antenna dimensions are in the order of a wavelength. Linear antennas of the dipole-type dominate this frequency band. In order to obtain moderate values of gain, some single elements have to be combined to form an array. Broadside arrays with individual feeding are used as well as endfire arrays of the Yagi-type, sometimes combined with some kind of reflector.

The first part of this paper deals with the optimisation of the linear single elements for maximum gain. It will be shown that the straight-lined dipole is an optimum solution only as long as its overall length does not exceed one wavelength $\lambda$. For longer linear antennas an optimum shape for maximum gain can be computed. Combining such optimum shaped elements results in new types of VHF- and UHF-arrays with surprising properties.

The second part of the paper is concerned with the noise contributions of receiving antennas. The active antenna concept is shown to be the optimum solution for maximum signal-to-noise ratio at the receiver output and this concept is also particularly helpful in cutting antenna dimensions at the lower frequencies.

## WIRELESS TRANSMISSION SYSTEM WITH PASSIVE ANTENNAS

### Basic Requirements

The signal-to-noise ratio $P_S/P_N$ at the output terminals of the receiver is a most important parameter in any wireless transmission system. The greater $P_S/P_N$, the greater is the flux of information that can be transmitted and the smaller is the error probability of the transmission. As a consequence, the parameters of a radio link should be optimised in such a way that with given limits of expenditure (e.g. antenna size) the signal-to-noise ratio will become a maximum.

Fig. 1 gives the situation for a wireless transmission system in free space with a passive receiving antenna. The transmitting antenna is fed by the signal generator with signal power P. Assuming a transmitting-antenna gain $G_T$, the power flux density S (Poynting's vector) at the receiving antenna will be

$$S = \frac{P}{4\pi d^2} G_T \quad . \qquad (1)$$

d is the distance between transmitting and receiving antenna, and $G_T$ is related to the isotropic radiator.

Neglecting losses within the passive receiving antenna and within the connection cable to the receiver, the signal power $P_{S2}$ at the output terminals of the receiver will be

$$P_{S2} = \frac{P}{4\pi d^2} G_T \frac{\lambda^2}{4\pi} G_A g \quad . \qquad (2)$$

$G_A$ is the gain of the receiving antenna, g the available power gain of the receiver.

Due to various noise sources (e.g. Ko (1)) the antenna will also receive noise power. This is taken into account in Fig. 1 by a noise source with available power $P_{NA}$ at the output terminals of the receiving antenna.

The inherent noise of the receiver is characterised by a noise source with available power $P_{NR}$ at its input terminals. The total noise power at the receiver output is given by

$$P_{N2} = (P_{NA} + P_{NR})\, g \quad . \qquad (3)$$

Combining equation (3) with equation (2) yields the signal-to-noise ratio at the output terminals of the receiver:

$$\frac{P_{S2}}{P_{N2}} = \left(\frac{\lambda}{4\pi d}\right)^2 \frac{P\, G_T G_A}{P_{NA}+P_{NR}} \qquad (4)$$

Given the receiving system and its distance from the transmitter, the signal-to-noise ratio will depend entirely on the product $PG_T$, sometimes called the equivalent radiated power ERP. Fig. 2 gives the ERP, which is necessary to produce $P_{S2}/P_{N2} = 1$, for a distance of 1 km between transmitting and receiving antenna under the assumption that the receiving antenna has low gain as e.g. a dipole and that there is no receiver noise ($P_{NR}=0$).

The values of $P_{NA}$ are mean values of ter-

7

restrial noise as found in Central Europe ((1) and (2)). The decrease of $P_{NA}$ with frequency is responsible for the frequency dependence of the ERP as shown in Fig. 2.

In many communication systems the ERP is limited to certain maximum values and the signal-to-noise ratio can be increased only by optimisation of the receiving side, in particular of the receiving antenna.

From equation (4) it is evident that there are only two ways of maximising $P_{S2}/P_{N2}$ for a given value of $P \cdot G_m$, namely increasing the gain $G_A$ of the receiving antenna or reducing the noise contribution $P_{NR}$ of the receiver. First the possibilities of maximising $G_A$ shall be discussed.

Linear smallband antennas of optimised shape

Basically there is no real limitation to the maximisation of the directivity or gain of an antenna as long as no further restrictions, such as size, costs or bandwidth have to be considered. In the following the main restriction imposed on the optimisation of antenna gain shall be antenna size, which to some degree is equivalent to costs, whereas bandwidth shall be considered later. Assuming lossless antennas, the terms directivity and gain (as related to the isotropic radiator) shall be considered synonyms.

For simplicity, antennas are treated in their transmitting state in the following; according to the theorem of reciprocity, the antenna gain is identical in the transmitting and in the receiving state.

As stated earlier in this paper, the antenna commonly used within the VHF/UHF domain generally consists of a number of straight-lined single dipoles. It seems obvious that an improvement of the overall directivity should start with the optimisation of the single radiator.

There is little to gain with symmetrical dipoles as long as their length does not considerably exceed $\lambda$. With all current elements approximately in phase, there is a destinct radiation orthogonal to the dipole axis. Antenna gain is 2.1 dB for the halfwave and approximately 3.8 dB for the fullwave dipole.

For dipoles longer than a wavelength the situation changes drastically as is shown in Fig. 3a, which gives a first approximation of the current on a straight-lined 1.5 $\lambda$-dipole. From the phase reversal within the current distribution it becomes evident that radiation normal to the dipole axis will be poor. As a consequence, dipoles which are considerably longer than one wavelength are scarcely used.

If properly shaped, however, a 1.5 $\lambda$-dipole as shown in Fig. 3b can be a very efficient radiator, which is superior in gain to conventional straight-lined dipoles. The basic idea is to compensate the phase differences within the current distribution by time delays. Due to a special shaping, waves originating from various sections of the antenna arrive at different times at a far-off point in the direction of main radiation (parallel to the plane of symmetry). The time delays correspond to phase shifts. For optimum shape of the antenna structure the resulting phase shifts will approximately compensate the phase reversals within the current distribution and the fieldstrength phasors in the farfield will add almost in phase. This is only true, however, in the deliberate direction of main radiation but will in general not hold for other directions. As a consequence, relatively high values of directivity can be expected with such an antenna.

The optimum shape of a dipole which is longer than a wavelength can be found in different ways (Landstorfer (3,4)). A straight forward method is to compute the radiation pattern of an arbitrarily shaped antenna, to calculate the directivity from the pattern data and change the antenna structure until a maximum is found.

Fig. 4 shows the upper half of a symmetrical linear antenna of arbitrary shape. $\zeta$ is the coordinate along the axis. The gain (or directivity) $G_A$ of this antenna can be calculated from the distribution of Poynting's Vector $S(\varphi,\vartheta)$, where $\varphi,\vartheta$ and r are spherical coordinates as shown in Fig. 4 and r=const.

$$G_A = \frac{4\pi\, S_{max}}{\iint S(\varphi,\vartheta)\, \sin\vartheta\, d\vartheta\, d\varphi} \qquad (5)$$

$S_{max}$ is the maximum of $S(\varphi,\vartheta)$ in the direction of main radiation.

Poynting's Vector $S(\varphi,\vartheta)$ is a real value as long as r=const. is large enough to ensure farfield conditions, and can be computed e.g. from the vector of the magnetic farfield fieldstrength $H(\varphi,\vartheta)$.

$$S(\varphi,\vartheta) = \frac{1}{2} \left| \vec{H}(\varphi,\vartheta) \right|^2 \cdot Z_o \qquad (6)$$

$Z_o$ is the field characteristic impedance of free space. With the denotation of Fig. 4

$$\vec{H}(\varphi,\vartheta) = K(r) \cdot \int_{\zeta=-L}^{L} \left[\vec{u}(\zeta) \times \vec{a}(\varphi,\vartheta)\right] \cdot \left\{ I(\zeta) \exp\left[\vec{c}(\zeta) \cdot \vec{a}(\varphi,\vartheta)\right] \right\} d\zeta \qquad (7)$$

$\vec{u}(\zeta)$ is a unity vector marking the direction in space of the antenna element and antenna current at $\zeta$; $\vec{c}(\zeta)$ is the position vector of $\zeta$ as seen from the origin and $\vec{a}(\varphi,\vartheta)$ is a unity vector with the spherical coordinates $\varphi,\vartheta$.

K is constant for r=const.

In order to facilitate the evaluation of the integral of equ. (7) two assumptions will be made:

a) The current distribution along the antenna is sinusoidal and will not change even if the antenna shape changes, as long as the arc-length 2L of the antenna remains constant.

b) The shape of the antenna of Fig. 4 can be approximated by n straight-lined sections of constant length $\Delta s$.

With these assumptions, the antenna shape as shown in Fig. 5 is given by n inclination angles $\alpha_1 \ldots \alpha_n$. Hence the integral in equ. (7) can be split into a sum of subintegrals over the different straight- lined sections. The subintegrals can be evaluated analytically and with equ. (5) and (6) the gain $G_A$ of the antenna can be computed as a function of $\alpha_1$ to $\alpha_n$.

$$G_A(\alpha_1, \alpha_2, \ldots \alpha_n) \qquad (8)$$

The integral in equ. (5) is evaluated by help of numerical methods (ref. (3)).

In order to find the optimum antenna shape for maximum gain, the function $G_A(\alpha_1 \ldots \alpha_n)$ has to be maximised. Quite a number of different mathematical methods are available for this purpose (see e.g. Adby and Dempster (5)). For the problem as stated above, the method of the steepest ascent proved to be very efficient.

Starting with an initial set of variables $\alpha_1$ to $\alpha_n$, the gradient of the function $G_A$ is computed, which points into the direction of the maximum increase. Then a search procedure yields the maximum of the function along this direction. At the locus of this relative maximum the gradient vector is computed anew and the procedure repeated until the maximum of $G_A$ is found.

The optimum shape of a symmetrical linear $1{,}5\lambda$-dipole ($L = 0.75\lambda$), which was found in this way and extrapolated for $n \to \infty$, is given in Fig. 3b. The calculated and measured gain for this radiator is 7.8 dB, which is a good value for a single element antenna.

Even higher values of gain can be obtained, if multiwire structures are used instead of a single wire. The result of a similar optimisation process as described above but applied to a two-wire structure is given in Fig. 6 for n = 6 sections and $L = 0.75\lambda$. As the two conductors follow spatial curves, the antenna must be represented in at least two views.

The computed and measured gain of the antenna of Fig. 6 (symmetrically completed) is around 1o.5 dB with respect to the isotropic radiator.

The optimisation process afore described can also be applied to linear structures of different arc-length (Landstorfer (6) and (7)). With respect to size, however, elements with $L \approx 0.75\lambda$ offer some advantages and will be dealt with exclusively, in the following.

As mentioned earlier, higher values of gain with antennas in the VHF/UHF-range are generally obtained by combining more than one element within an array. A most succesful and widely used antenna of this type is the Yagi-Uda array with one driven element and a number of parasitic directors and reflectors. Due to the relatively low directivity of a single straight-lined dipole, quite a number of elements are necessary in a conventional Yagi-Uda array in order to get some moderate values of gain.

It seems attractive to exploit the remarkable directivity of the optimum shaped antennas of Figs. 3b and 6 for designing new types of radiation-coupled arrays with a small number of elements.

As an example Fig. 7 shows a 3-element array with a driven radiator according to Fig. 3b and two optimised parasitic elements acting as reflector and director. In principle, the shape of these parasitic elements can also be found by optimisation techniques. The computational work envolved in such a task is considerable, however, and it is time saving to follow the customary line of Yagi optimisation by empirics. So with the antenna of Fig. 7, the central and driven radiator given, the parasitic elements were found by experiment.

Fig. 8 shows the E- and H-plane pattern of the antenna of Fig. 7. The measured gain is 11.5 dB. In order to give a comparison of size, Fig. 9 shows the optimised antenna of Fig. 7 together with a conventional UHF-Yagi with corner reflector. In the E-plane the beamwidth of both antennas is approximately identical; due to its large extension, the beam-width of the conventional Yagi is smaller in the H-plane but again almost the same value can be obtained if two optimised Yagis are stacked. Still more important e.g., if the antenna is used for TV-reception, is the large value of sidelobe attenuation, which is better than 20 dB, and a front-to-back ratio of 26 dB. Field tests over more than three years confirmed the theoretical results in practice.

As bandwidth was not a decisive parameter for the optimisation process, the bandwidth of the antenna of Fig. 7 is expected to be small. Indeed, as the relatively high directivity is due to some phase relations, which are frequency dependent, the antenna gain is frequency dependent too. Tolerating a decrease of gain at the band limits of o.5 dB, the relative bandwidth is 2.5 %; with a 3 dB reduction the bandwidth is 8 %. Of course, the input impedance of the antenna also depends on frequency and determines the useful bandwidth of the array. Impedance matching is satisfactory, however, within the band limits as determined by the radiation pattern.

The optimised shape of Fig. 6 was also used in experiments with 3-element Yagi arrays. The measured gain of such a 3-dimensional array is around 13.6 dB.

Another promising application of the radiator of Fig. 6 is its combination with a circular reflector as shown in Fig. 10. The optimised radiator of Fig. 6 is oriented in such a way that its direction of main radiation points to the reflector. Reflector antennas of this type are generally called "Short Backfire" and were first described by Ehrenspeck (8). The Backfire as shown in Fig. 10 differs from conventional ones by using an optimum shaped primary radiator. With a diameter of the reflector of $2\lambda$, a gain of 15.5 dB was measured. Due to the special shape of the feeder, its phase centre moves toward the reflector with increasing frequency. Thus - in terms of wavelength - the distance between feeder and reflector surface remains more constant with this antenna than with conventional Backfire structures and the gain shows a relatively small frequency dependence.

## Logarithmic-Periodic Arrays

The antenna of Fig. 10 is a first step from smallband antennas to antennas designed for larger bandwidths. The classical approach to a broadband design with VHF/UHF antennas is the logarithmic-periodic array consisting of a number of straight-lined dipoles. These antennas, if properly designed, offer excellent broadband capability; their directivity is rather limited, however. As the single radiators shown in Figs. 3b and 6 offer values of gain which are considerably higher than those found with straight-lined dipoles, it seems promising to combine the broadband behaviour of the log-periodic principle with the high directivity of optimum shaped dipoles.

Fig. 11 shows schematically a log-periodic array of optimum shaped dipoles according to Fig. 3b.

Conventional logarithmic-periodic arrays generally are described in terms of the included angle $\alpha$ and of the parameter $\tau$ . In analogy, these parameters can also be applied to log-periodic antennas with optimised elements as shown in Fig. 11.

$$\tau = l_{n+1}/l_n \qquad (9)$$

In contrast to conventional log-periodic arrays, the paramter $\tau$ has to be chosen very carefully when using optimised structures as the bandwidth of the latter ist smaller than with straight-lined halfwave dipoles. Fig. 12 gives the input impedance of the single optimised radiator of Fig. 3b near resonance. Taking a VSWR of 2 (dashed curve in Fig. 12) as the bandwidth limit, the relative impedance bandwidth is at least 13 %. As a 1 dB decrease of radiation gain occurs with a relative bandwidth $b_r$ = 6 % already, the frequency dependence of the radiation pattern determines the useful frequency range for the single radiator.

In order to cover a continuous frequency range with the log-periodic antenna, the frequency ranges covered by the individual elements should either overlap or adjoin on each other. From this condition follows:

$$\tau = (2 - b_r)/2 + b_r) \qquad (10)$$

The included angle $\alpha$ determines the number of elements needed for a specified frequency range. As a general rule, small values of $\alpha$ give a large number of elements with the advantage of high directivity. On the other hand, the number of single radiators can be reduced with larger included angles at the sacrifice of gain, however.

Fig. 13. shows as one of many existing examples a 6-element log-periodic array with optimised radiators according to Fig. 3b for the frequency range 470... 610 MHz. $\tau$ is o.94 and $\alpha = 20^0$. The average gain was measured around 12.5 dB.

Fig. 14 gives the E-plane radiation pattern for the antenna of Fig. 13. The pattern is typical and does not change very much with frequency as is customary with conventional log-periodic arrays.

The same average gain was achieved with a 3-element antenna covering the frequency range from 370 to 470 MHz with $\tau$ = o.87 and $\alpha = 60^0$.

The gain optimised radiator of Fig. 6 is used as an element in the log-periodic antenna of Fig. 15. Due to the higher directivity of the single element, the average gain of this antenna is in the order of 16 dB. The parameters are $\tau$ = 0.94 and $\alpha = 40^0$ and the frequency range 470 to 610 MHz.

Experiments with this type of antennas are still under way; in particular, arrays with more elements and larger frequency bands are being tested at the moment. First results indicate that considerably higher values of gain are feasible with log-periodic arrays using the concept of gain optimised elements.

## ACTIVE ANTENNAS

Maximising the gain $G_A$ of the receiving antenna in general means increasing the signal power $P_{S2}$ in equations (2) and (4) but does not necessarily mean that $P_{N2}$ in equations (3) and (4) ist not affected. With an <u>isotropic</u> distribution of the incident noise power density, $P_{NA}$ in equations (3) and (4) will not change, and unless the matching conditions at the input of the receiver are changed, its noise contribution $P_{NR}$ will also remain constant. Hence the signal-to-noise ratio at the receiver output will increase proportionally with the gain $G_A$ of the receiving antenna.
For incident noise radiations from directions which differ remarkably from the direction of main reception of the antenna, an increase in directivity can help to eliminate noise sources and $P_{S2}/P_{N2}$ will grow super-proportionally with gain $G_A$. There is only one case where an increase in receiving gain will not change the signal-to-noise ratio, that is when noise and signal are received from the same direction. This situation is scarce, however.

An alternative and sometimes additional method to maximising the numerator in equ. (4) is to minimise the denominator. As the contribution $P_{NA}$ of the external noise sources to the overall noise $P_{N2}$ in general cannot be changed, a minimisation of $P_{N2}$ can only be achieved by reducing the noise contribution $P_{NR}$ of the receiver. This can be accomplished by the concept of the active antenna.

Active antennas have first been investigated at Ohio State University (9); the first antennas for field use, however, have been developed after intensive research programmes at the Institute for RF-Frequency Techniques of the Technical University of Munich (1o...15).

The basic concept of the active antenna is shown in Fig. 16. The first amplifying stage is not found within the receiver but is integrated with the antenna structure (e.g. a bipolar transistor as shown in Fig. 16). As a consequence, the signal power $P_{S2}$ at the output terminals of the receiver is increased by the available power gain $g_{tr}$ of the transistor.

$$P_{S2} = P \left(\frac{\lambda}{4\pi d}\right)^2 G_T G_A g_{tr} \qquad (11)$$

Assuming the output of the active antenna to be matched to the characteristic impedance $Z_L$ of the connection cable, the noise $P_{NR}$ of the receiver will not change and the total noise power at the output terminals of the receiver will become

$$P_{N2} = (P_{NA} + P_{Ntr})g\, g_{tr} + P_{NR}g \,. \qquad (12)$$

$P_{Ntr}$ is the noise contribution of the active element integrated with the antenna. Hence the signal-to-noise ratio is

$$\frac{P_{S2}}{P_{N2}} = \left(\frac{\lambda}{4\pi d}\right)^2 \cdot \frac{PG_TG_A}{P_{NA}+P_{Ntr}+P_{NR}/g_{tr}} \qquad (13)$$

For sufficiently high values of the power gain $g_{tr}$ the noise contribution of the receiver becomes negligible and is replaced by the noise contribution of the active element e.g. the transistor in Fig.16.

As has been proved elsewhere (13), $P_{Ntr}$ can be smaller than $P_{NR}$ in equ. (4) even if identical types of active elements are used in the first stage of the receiver and in the active antenna. In the case of the conventional "passive antenna-receiver" configuration of Fig. 1, the absolute minimum for the noise contribution $P_{NR}$ cannot be achieved since the input of the receiver has to be "power-matched" to the connection cable. For the "active antenna" concept of Fig. 16 this limitation does not apply and the principle of "noise-match" can fully be exploited. Thus the absolute minimum noise figure which is feasible with the type of simiconductor used can be obtained and the denominator in equ. (13) becomes a minimum.

At lower frequencies, where the external noise level ($P_{NA}$) is rather high, the low-noise property of the active antenna can be exchanged for a reduction in antenna size. As a basic rule, $P_{Ntr}$ can be allowed to be in the same order as $P_{NA}$ without deteriorating the optimum signal-to-noise ratio remarkably.

Two examples of active antennas which have been designed at the Technical University in Munich are given in Figs. 17 and 18.

Fig. 17 shows an array of two active antennas for a helicopter homing-system. In comparison with an earlier system, which used passive antennas, the 50 cm active dipoles are smaller by a factor of 3. The frequency range covered is from 30 MHz to 87 MHz but could easily by extended to larger bandwidths. The signal-to-noise ratio with the active antenna system is generally better or at least equal to that obtained with the passive system (identical receivers presupposed).

Active antennas are the only means to cover extremely large bandwidths without loss of sensitivity. As an example, Fig. 18 shows an active antenna for the frequency range from 100 kHz to 1 GHz.

Of course, best results of signal-to-noise ratio are obtained by the combination of maximised directivity and minimised noise, as is e.g. the case for the Yagi of Fig. 7 with integrated, noise-matched amplifier.

REFERENCES


1. Ko, H.C., 1958, Proc. IRE. 46, 208-215.
2. CCIR-Report, 1959, CCIR, 65, 223-256.
3. Landstorfer, F., 1978, Kleinheubacher Berichte, 21, 87-93.
4. Landstorfer, F., 1977, Symposium Digest CAD of Electronic and Microwave Circuits and Systems, Hull, 96-101.
5. Adby, P., and Dempster, M., 1974, "Introduction to Optimizations Methods", Chapman and Hall, London.
6. Landstorfer, F., 1976, "On the optimum shape of linear antennas", Symposium Digest, IEEE Symp. AP, Amherst, Mass., 167-172.
7. Landstorfer, F., 1976, Frequenz, 30, 344-249.
8. Ehrenspeck, H., 1960, Proc.IRE, 49, 109-110.
9. Copeland. J., Robertson. W., and Verstraete, R., 1964, Trans. AP, 12, 227-233.
10. Meinke, H., 1966, Radio & Electron. Eng. 31, 76-80.
11. Lindenmeier, H., 1967, "Kurze aktive Empfangsantennen", PhD-Thesis, TU-München.
12. Meinke, H., 1966, Nachrichtentechn. Z., 19, 697-705.
13. Lindenmeier, H., 1969, Nachrichtent.Z., 22, 381-389.
14. Landstorfer, F., 1969, Nachrichtent.Z., 22, 694-700.
15. Flachenecker, G., Landstorfer, F. Lindenmeier, H., and Meinke, H., 1972, de Ingenieur, 84, ET 74-80.

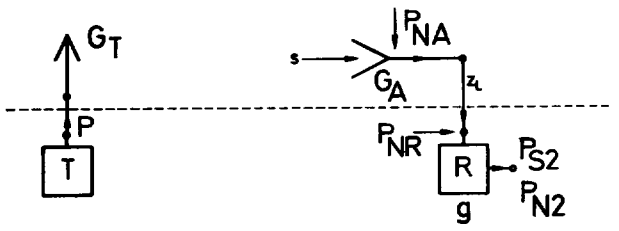


Figure 1 Wireless transmission system with passive antennas

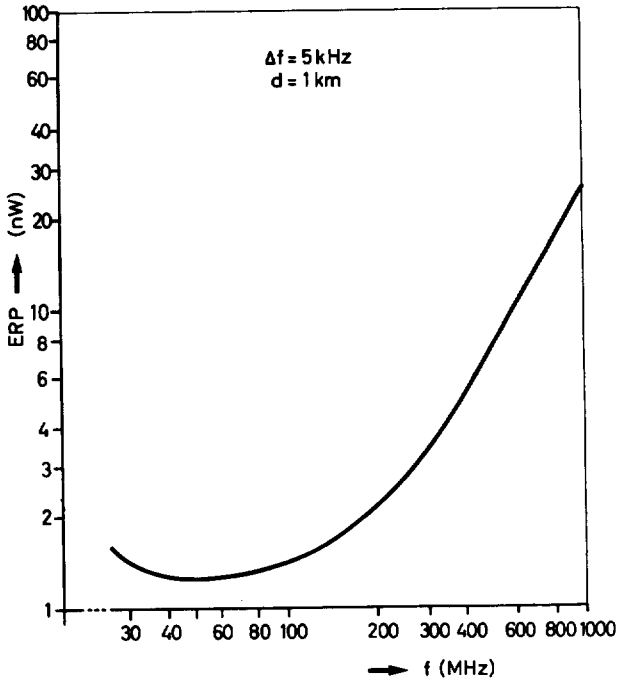


Figure 2 ERP for the system of Figure 1 and a signal-to-noise ratio of 0 dB at the output of the receiver

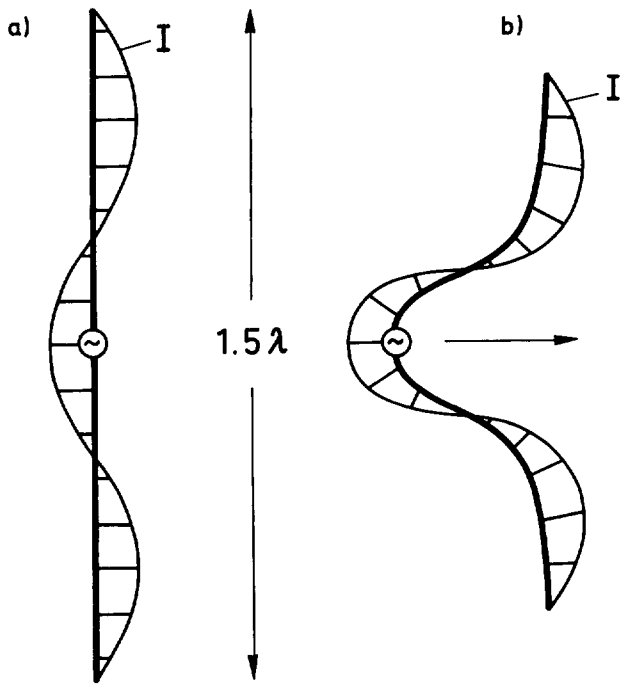


Figure 3 Approximation of the current distribution on a) a 1,5-λ dipole and b) a dipole with gain-optimised shape

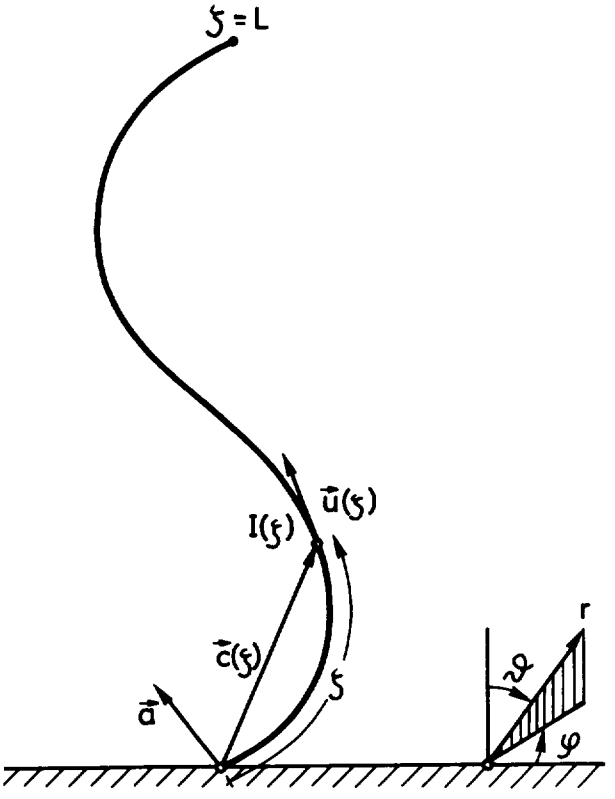


Figure 4 Linear antenna of arbitrary shape

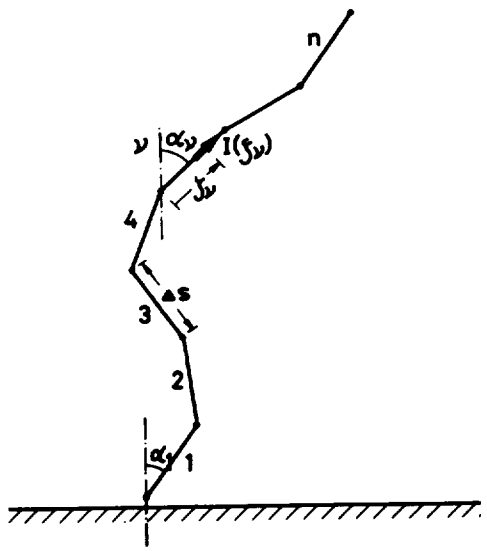


Figure 5 Linear antenna of arbitrary shape with n straight-lined sections

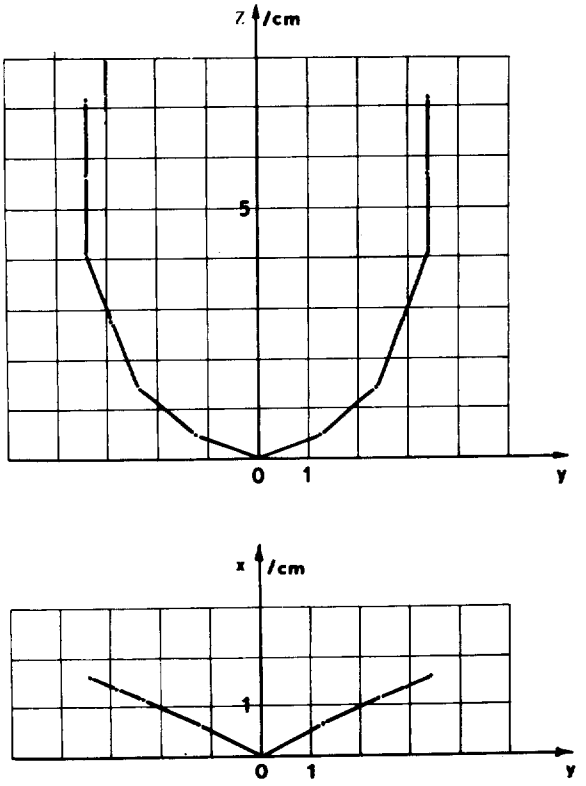


Figure 6 Dual-wire antenna of optimised shape; L = 0.75 $\lambda$ .

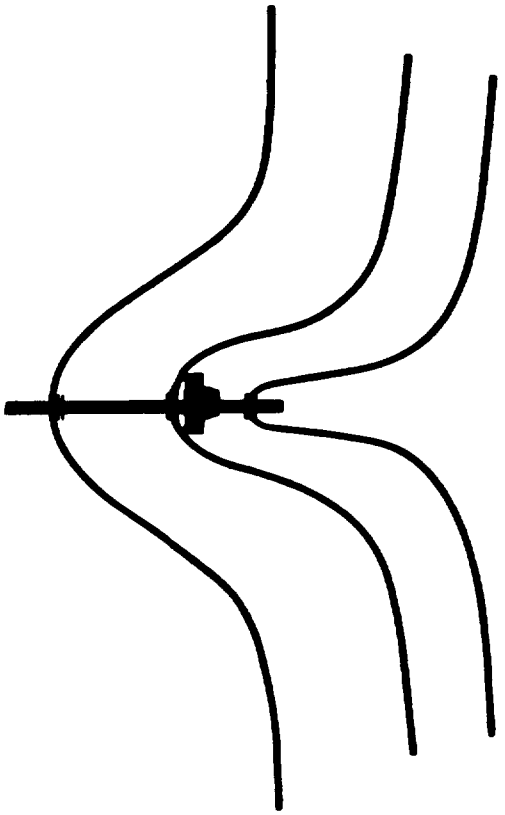

Figure 7 Yagi-array with 3 gain-optimised elements

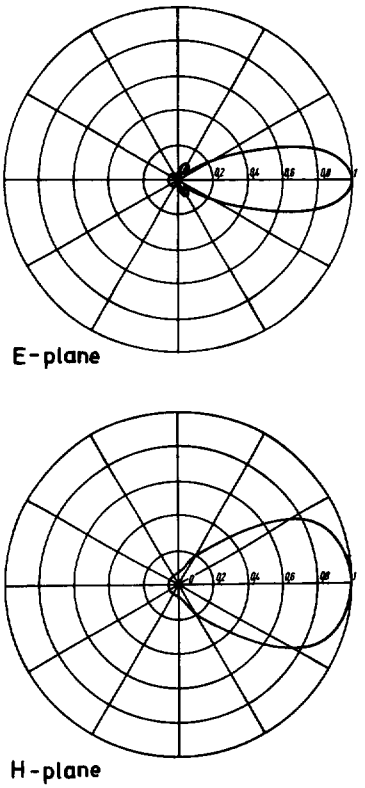


Figure 8 E- and H-plane pattern of the antenna of Fig. 7

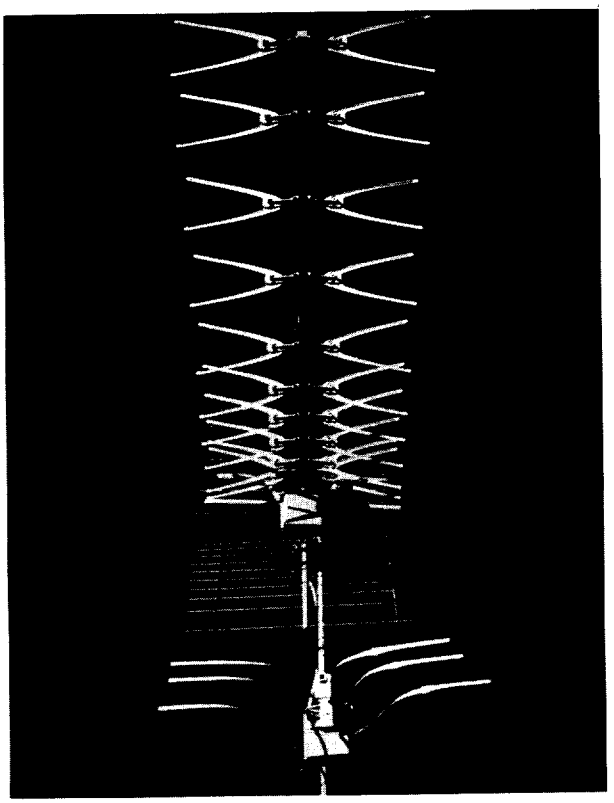

Figure 9 Conventional and gain-optimised Yagi

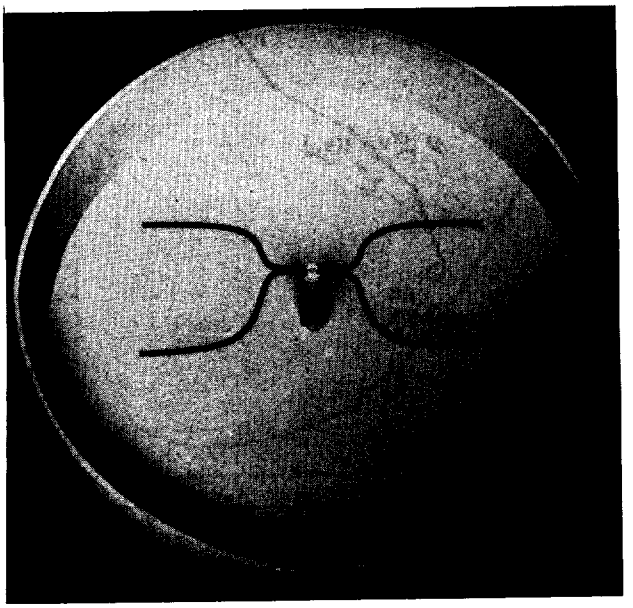

Figure 10 New Type of backfire antenna with optimised feeder

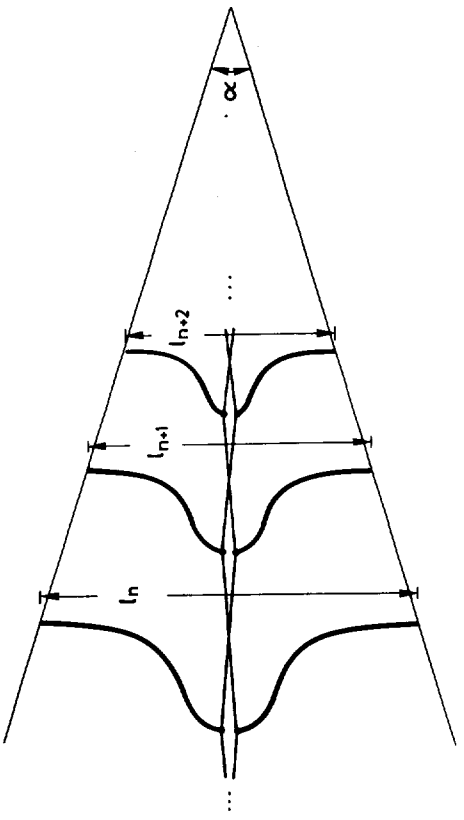


Figure 11 Log-periodic array

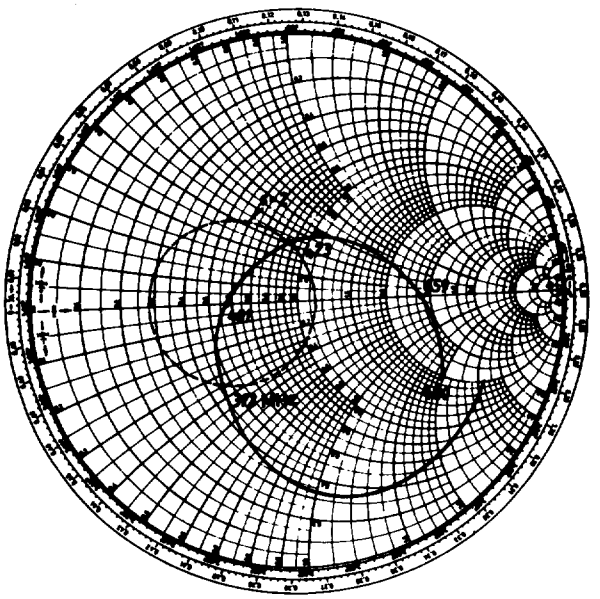


Figure 12 Impedance of a single element radiator

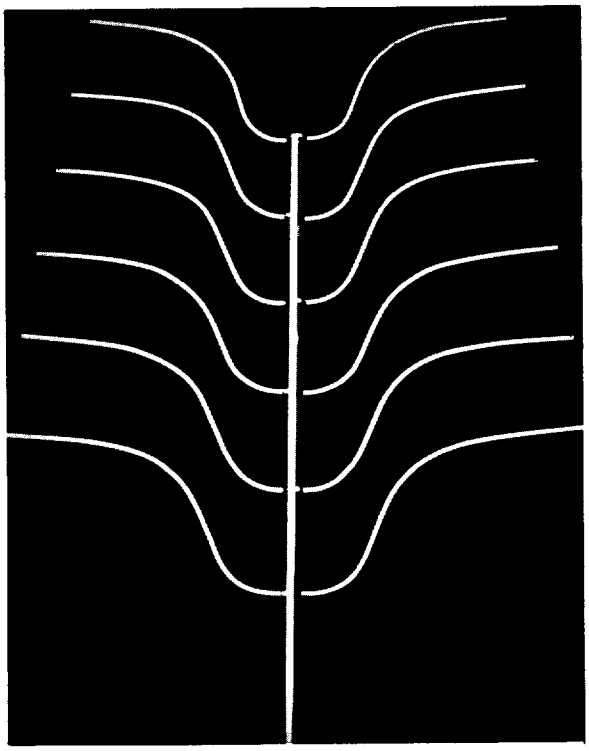

Figure 13 Log-periodic array with 6 elements of optimised shape

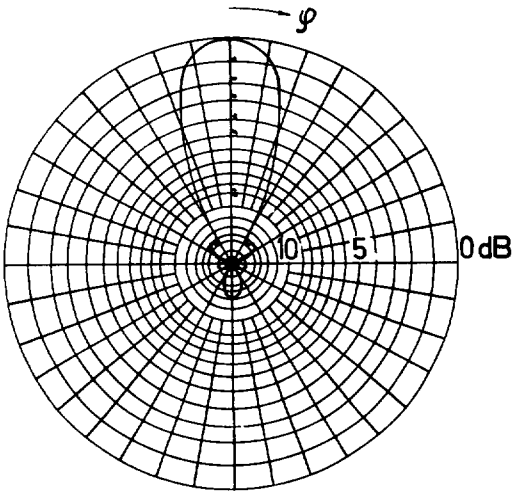


Figure 14 E-plane pattern of the antenna of Fig. 13

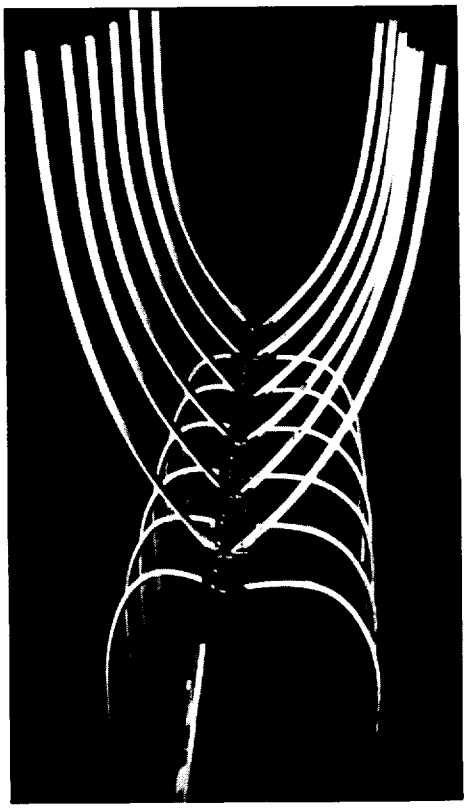

Figure 15 Log-periodic array with 6 single elements according to Fig. 6

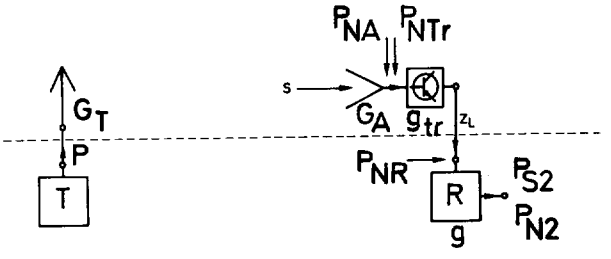


Figure 16 Wireless transmission system with active receiving antenna

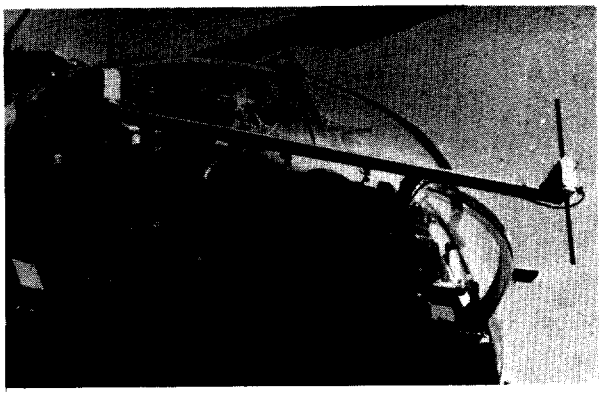

Figure 17 Array of two active antennas for a helicopter navigation system

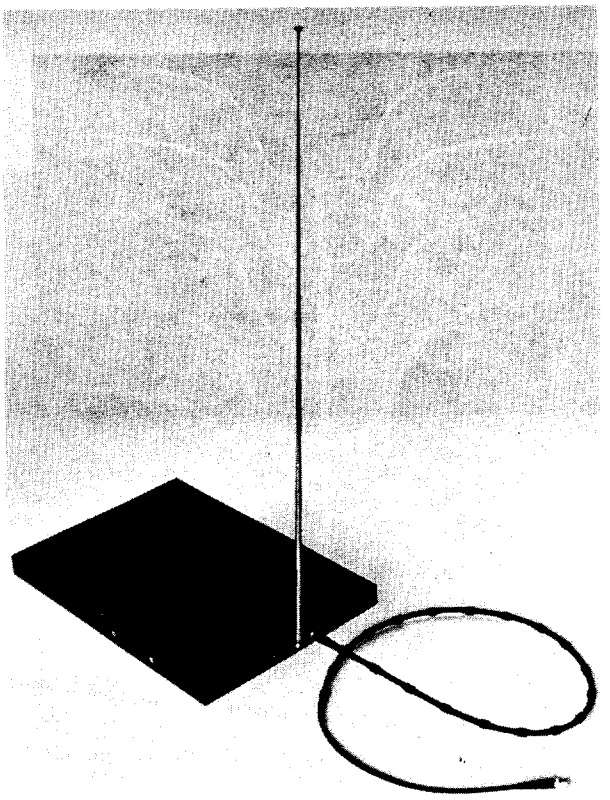

Figure 18 Active broadband antenna 100 kHz-1GHz